The Astrophysical Journal, 630:L41–L44, 2005 September 1
© 2005. The American Astronomical Society. All rights reserved. Printed in U.S.A.

DEUTERIUM ABUNDANCE IN THE INTERSTELLAR GAS OF THE GALACTIC ANTICENTER FROM THE 327 MHz LINE

A. E. E. Rogers, K. A. Dudevoir, J. C. Carter, B. J. Fanous, and E. Kratzenberg
MIT Haystack Observatory, Westford, MA 01886-1299; arogers@haystack.mit.edu
and
T. M. Bania
Institute for Astrophysical Research, Boston University, 725 Commonwealth Avenue, Boston, MA 02215
Received 2005 May 25; accepted 2005 July 19; published 2005 August 12

ABSTRACT

The deuterium abundance in the primordial gas formed during the big bang is dependent on the baryon-to-photon ratio during nucleosynthesis. We report a measurement of the deuterium-to-hydrogen (D/H) ratio from a 6 σ detection of the hyperfine ground-state transition of deuterium at 327 MHz (92 cm) in emission from the interstellar gas in the region of the Galactic anticenter. We find the maximum signal at $l = 183°$, where the deuterium line opacity is expected to be a maximum as a result of velocity crowding. Using these deuterium and existing hydrogen observations, we model the effects of beam dilution, spin temperature, and absorption of continuum to derive a D/H ratio of $2.3^{+1.5}_{-1.3} \times 10^{-5}$ by number. The errors are $\pm 3\,\sigma$ plus our estimate of the systematic uncertainty in the conversion of the observed line amplitude to the D/H ratio.

Subject headings: cosmology: observations — Galaxy: general — ISM: abundances — radio lines: ISM — techniques: spectroscopic

1. INTRODUCTION

Following the detection of the 1420 MHz (21 cm) hyperfine transition of hydrogen (Ewen & Purcell 1951) and its use in the mapping of the interstellar gas in the Galaxy, the search for the similar ground-state spin-flip transition of deuterium at 327 MHz (92 cm) was urgently pursued as a means to constrain the photon-to-baryon ratio based on the theory of nucleosynthesis during the big bang (Burles et al. 2001). Estimates of the deuterium-to-hydrogen (D/H) abundance ratio from the ultraviolet Lyα lines have differed by more than a factor of 2. While most of the differences are now thought to be the result of astration and the depletion of D by attachment to interstellar grains (Draine 2004), the small isotopic wavelength shift for the UV D transition could lead to systematic errors due to line blending with high-velocity H. The radio transition of D is well separated from other lines with which it might be confused. However, the D line's amplitude is extremely weak; most observers have only been able to set an upper limit on the D/H ratio. Weinreb (1962) set an upper limit of 8×10^{-5} by looking for the 327 MHz line in absorption in the spectrum of the radio source Cassiopeia A. Anantharamaiah & Radhakrishnan (1979) set an upper limit of 5.8×10^{-5} for the line in absorption in the Galactic center and discuss earlier attempts to detect the line toward the Galactic center (Cesarsky et al. 1973; Pasachoff & Cesarsky 1974). Blitz & Heiles (1987) looked for the line in emission toward the Galactic anticenter and set an upper limit of 6×10^{-5}. Heiles et al. (1993) set a limit of 5×10^{-5} from observations of the Galactic center and Cassiopeia A. Chengalur et al. (1997) obtained a marginal detection of the emission from the anticenter to place the D/H ratio between 2.9×10^{-5} and 4.9×10^{-5}.

2. INSTRUMENT DESCRIPTION

2.1. *Array for* 327 MHz

Since the hydrogen emission from the anticenter is extended over many degrees and has high optical depth, we built an array (Table 1) of relatively small electronically steered antennas to optimize the sensitivity for the detection of the deuterium line. Each "station" consists of a linear 5 × 5 (minus one corner element) subarray of 24 active crossed Yagi elements with 0.8 wavelength spacing on a 4.8 × 4.8 wavelength horizontal ground plane. The Yagis have directors optimized to minimize the gain at the horizon in order to reduce the sensitivity to interference, which mostly comes from the horizon. The beamwidth formed by each station is approximately matched to the extent of the expected deuterium emission. The spectra from the 24 stations are averaged to provide a 24-fold increase in the equivalent integration time compared with that of a single station. Low-noise amplifiers (LNAs) are directly connected to the antenna elements, which also form stub filters to reduce the signal levels from FM, TV, and an adjacent digisonde transmitter, which can generate intermodulation products in the LNA. The amplified outputs are filtered and downconverted to a 50 MHz intermediate frequency, which is then digitized and downconverted to baseband. The combination of analog and digital filtering provides over 100 dB rejection of out-of-band signals. The digital baseband outputs from the antenna elements are converted to spectra, using 1024-point complex fast Fourier transforms, and summed, with appropriate phasing, to provide four simultaneous beams in each polarization. The power spectra from each beam and each antenna element are accumulated and written to disk every 500 s.

2.2. *Radio Interference Detection and Reduction*

To prevent any signals from the electronics coupling into the antennas, the station receivers are shielded in closed boxes with filtered AC power and fiber optics for communications. A separate radio-frequency interference (RFI) monitoring system consisting of 12 active Yagi antennas pointed every 30° in azimuth is used to detect sources of interference in our 250 kHz observing band centered at 327.4 MHz (Rogers et al. 2005). This band is within the 322.0–328.6 MHz radio astronomy band, which is shared with government services. There are no fixed transmitters assigned in this band within 50 km of the array, but there are transient signals, such as

TABLE 1
SUMMARY OF ARRAY CHARACTERISTICS

Characteristic	Value
Location	Haystack Observatory, Westford, MA; latitude N42.°6, longitude W71.°5
Array configuration	Quasi-regular array of 24 stations
Station separation	Approximately 15 m
Station antenna	Compact array of 24 crossed Yagis
Station collecting area	12 m^2
Station beamwidth	14°
Electronic beam steering	±40°
Frequency center	327.4 MHz
Frequency span	250 kHz
Number of spectral channels	1024
Resolution	244 Hz
Polarization	Dual linear
System temperature	40 K plus sky noise
Number of receiver ports	48 × 24 = 1152

occasional unwanted out-of-band emissions from mobile and aeronautical transmitters. These RFI emissions are detected by the monitoring system and then excised from the data.

Continuous-wave (CW) RFI is present from personal computers, digital answering machines, and other electronics in surrounding observatory buildings and adjacent residences. Many of these sources have been located and reduced by shielding or removed. The effect of the remaining signals is mitigated by the exclusion of their frequencies. Since these signals are much narrower than the expected 20 kHz width of the D line, their exclusion only slightly degrades the signal-to-noise ratio (S/N) of the estimate of the D line's strength. The Yagi antennas of the RFI monitor have a gain of 13 dBi, while the horizon response of array Yagis is about −10 dBi, so that a CW signal with S/N less than 6 from the RFI monitor results in an equivalent signal of less than about 1 part per million (ppm) in the station-beam data. This reduces the effect of RFI that is not detected by the monitor to a level well below that expected from the D line.

3. OBSERVATIONS AND DATA REDUCTION

3.1. *Observing Schedule*

The array runs an automated schedule with three of the four simultaneous beams tracking Galactic longitudes 171°, 183°, and 195° and the fourth beam pointed at the zenith. When the anticenter regions are below 50° elevation, other regions at the same declinations but shifted by 6^h, 12^h, and 18^h are observed for reference. The Sun, the peak of the continuum in the region of Cygnus, and the pulsar 0329+54 are also observed for short periods each day to provide checks on the phasing of the antenna elements. The primary method of intensity calibration is from the comparison of the zenith-pointed beam with a sky model (Rogers et al. 2004). Five hours of observation of the longitudes 171° and 183° and about 3 hours at 195° are obtained each day. Only observations with scan angles less than 40° are scheduled, since the aperture efficiency drops below 50% beyond this angle.

3.2. *Maximum Likelihood Estimation of the Line Amplitude*

The spectra from each polarization of each station are averaged each day. Transient signals with S/N greater than 6 in any RFI monitor or array antenna are excised from this average. The amplitude of the D line is estimated from a least-squares fit of all the data for a given source region to determine a separate constant for each station each day and a common amplitude of the expected profile. We simplified the data analysis by obtaining the maximum likelihood estimate for all the data toward a given region from the weighted average of the individual daily estimates for each station and polarization. The conversion from frequency to LSR is made each day based on a rest frequency of 327.384352 MHz (Wineland & Ramsey 1972). The reference regions were corrected to the LSR of the corresponding region in the Galactic plane at the same declination so that the reference regions were treated in the same way as the regions in the plane. The weighting for each spectral point of each daily average for each station is proportional to the integration time but is set to zero for any frequencies that exceed a S/N of 6 in the RFI monitor or in the average of the array antennas. The 1 σ noise in the final estimate is $\sigma = [\sum 1/\sigma_k^2]^{-1/2}$, where $\sigma_k = C_k^{1/2}(BT_k)^{-1/2}$, obtained from the covariance C_k of the estimated line-profile amplitude from the daily average spectra of each station, B is the resolution of 244 Hz, and T_k is the integration time in seconds. The 1 σ noise approximately equals $(wT)^{-1/2}$, where w is the width of the line profile in hertz and T is the "equivalent single station" integration time in seconds.

TABLE 2
MAXIMUM LIKELIHOOD ESTIMATES OF DEUTERIUM LINE STRENGTH

l (deg)	b (deg)	Amplitude	S/N	Integration (yr)
171	0	1.9	3.3	7.2
183	0	3.9	5.8	6.5
195	0	2.2	2.2	3.1
181	69	−0.6	0.9	7.1
61	33	0.4	0.6	6.5
104	−23	0.4	0.6	6.2
213	77	−0.3	0.5	6.5
52	24	−1.0	1.6	5.9
107	−35	1.4	2.1	6.6
268	77	0.6	0.7	4.5
44	14	−0.9	1.0	3.5
112	−46	0.1	0.1	1.5

NOTE.—The integration time is the "equivalent integration time" (see § 3.2), which is the time a single station with one polarization would take to acquire the same amount of data acquired by the dual-polarized 24-station array (during the period from 2004 June 29 through 2005 April 29) after accounting for the loss of data due to RFI excision.

We list in Table 2 the results of maximum likelihood estimates for the D-line amplitude for observations made over a period of 10 months (2004 June 29 through 2005 April 29). We include reference regions out of the Galactic plane for which no D line is expected.

We made an alternative analysis in which we first smoothed the spectrum from each station for each day and each polarization with a weighted least-squares fit to the original spectrum with the excluded frequencies unweighted. We then derived a small baseline slope and curvature correction using the reference regions and applied it to all the data. The final spectrum for a given source region was obtained from the weighted average of the individual smoothed spectra corrected each day to the LSR for each region. We find that the two methods of analysis give the same D-line amplitude to within a few percent.

The Galactic anticenter source toward $l = 183°$ is our most significant detection of the 327 MHz D transition. Figure 1*a* shows this average D spectrum together with the least-squares

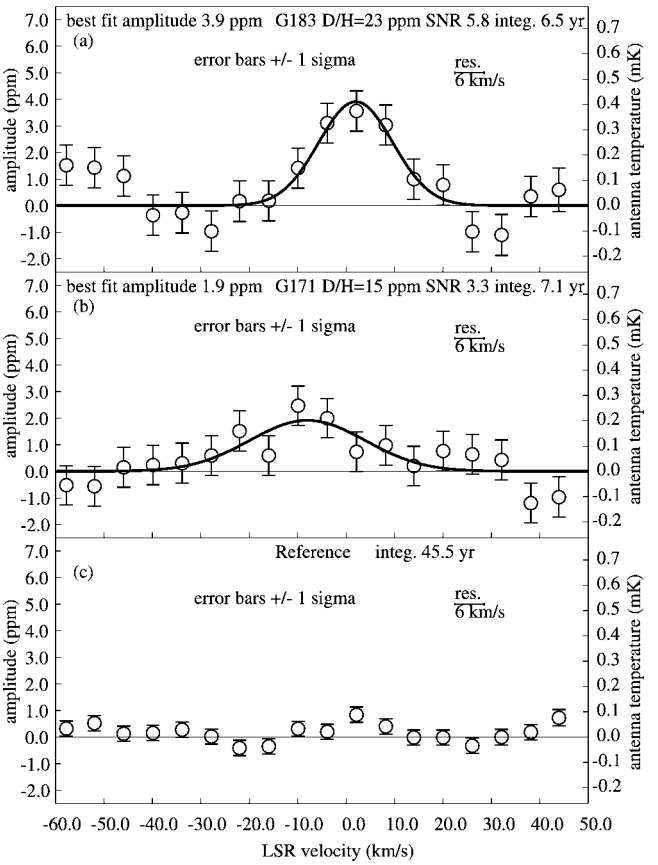

FIG. 1.—(*a*) Average D spectrum for the $(l, b) = (183°, 0°)$ direction. A S/N of 5.8 was calculated for the best-fit D line profile with width of 18 km s^{-1} and LSR velocity of 2 km s^{-1} from the line profile of Fig. 2*d*. The 1 σ bars shown on the plots are for the smoothed spectra with resolution of 6 km s^{-1}. (*b*) Average D spectrum for the $(l, b) = (171°, 0°)$ direction with the best-fit line profile, with width of 28 km s^{-1} and velocity of -8 km s^{-1}. (*c*) Average D spectrum for the reference regions, which are all at high Galactic latitude. An amplitude scale, which is the ratio of the signal to the system noise, and antenna temperature scale, based on an average system noise of 105 K, are shown. The integration time given here and in Table 2 is the "equivalent single-station integration."

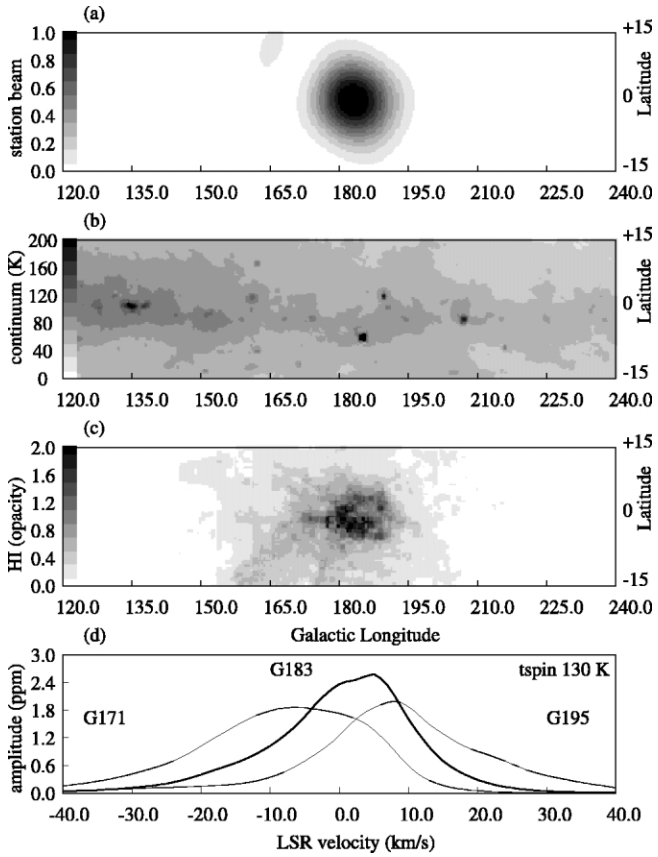

FIG. 2.—Estimated deuterium line profiles. (*a*) The station beam pattern toward $(l, b) = (183°, 0°)$. (*b*) Continuum emission in the anticenter region from Haslam et al. (1982). (*c*) H I opacity (for LSR velocity 0 km s^{-1}) in the anticenter region based on an assumed spin temperature of 130 K from Hartmann & Burton (1997). (*d*) Estimated D line profiles from beams toward $l = 171°$, 183°, and 195° using the convolution method described in the text. The entire data cubes of the continuum and H I data were used in these calculations.

fit to the expected line profile. Since we know the expected line velocity and width (see § 3.3), the S/N of 5.8 results in a formal probability of false detection given approximately by $(2\pi)^{-1/2}(\mathrm{S/N})^{-1}e^{-(\mathrm{S/N})^2/2}$, or about 3×10^{-9}. To gain added confidence in the result, we divided the anticenter data into equal parts and analyzed each data set separately. Each shows a D signal with a S/N > 3. Finally, our reference regions lie far off the Galactic plane and should not show any D emission. Figure 1*c* shows the average spectrum of the reference regions. The lack of any D signal at levels below that of the anticenter detection sets an encouraging limit on systematic instrumental effects that might produce a spurious detection.

3.3. *Simulation of Expected Deuterium Line Profiles*

The expected D line profile we used in the line amplitude analysis is derived from the H I and continuum emission data using a model. Figure 2 summarizes our method. Shown are maps of the station beam (Fig. 2*a*), the continuum emission (Fig. 2*b*) from Haslam et al. (1982) extrapolated to 327 MHz assuming a spectral index of 2.7, and the H I opacity (Fig. 2*c*) derived from the H I brightness from Hartmann & Burton (1997). The ratio of opacities (τ_D/τ_H) is equal to 0.27(D/H), where the factor 0.27 is derived from the ratio of the Einstein *A*-coefficients and the statistical weights with some small corrections (Gould 1994) to the values given by Field (1958). We assume that H and D have the same spin temperature (Field 1958) and the same velocity width, since turbulence is the dominant source of the Doppler broadening.

A model for the expected line velocity profile *p*, which accounts for beam dilution, is derived by the convolution of the antenna beam, *B*, with the expected line brightness $s(v, l, b)$, which is a function of velocity v, Galactic longitude l, and Galactic latitude b, We normalize with the continuum brightness $T_{\mathrm{cont}}(l, b)$ plus the receiver noise temperature, T_R, so that

$$p = (s \otimes B)/\{[T_{\mathrm{cont}}(l, b) + T_R] \otimes B\}, \quad (1)$$

where

$$s(v, l, b) = 0.27(\mathrm{D/H})[T_{\mathrm{spin}} - fT_{\mathrm{cont}}(l, b)]\tau_{\mathrm{H}}(v, l, b). \quad (2)$$

Here f is the fraction of continuum behind the interstellar gas and $\tau_{\mathrm{H}}(v, l, b)$ is the hydrogen opacity derived from the hydrogen line brightness using

$$\tau_{\mathrm{H}}(v, l, b) = -\ln[1 - T_{\mathrm{H}}(v, l, b)/T_{\mathrm{spin}}]. \quad (3)$$

Table 3 gives the expected peak of the line profile for a range of assumed spin temperatures and locations of the continuum emission. Here we assume a fiducial D/H ratio of 1.5×10^{-5}. The most reasonable assumption of a 130 K spin temperature and uniform mixing of the Galactic continuum (French & Osborne 1976) results in a peak line profile for the array observations toward $l = 183°$ of 2.6 ppm. The modeled profiles toward 171° and 195° have peak values of 1.9 and 2.0 ppm, respectively.

TABLE 3

EXPECTED D I PEAK LINE AMPLITUDE FOR $(l, b) = (183°, 0°)$

T_{spin} (K)	Amp.[a] (ppm)	Amp.[b] (ppm)	Amp.[c] (ppm)
110	1.7	3.2	4.7
120	1.7	2.9	4.1
130	1.6	2.6	3.6
140	1.6	2.6	3.6
150	1.7	2.4	3.2

NOTE.—Amplitude is the ratio of the signal to system noise. Assumes D/H = 1.5×10^{-5}.

[a] Continuum all behind H I.

[b] Continuum uniformly mixed with H I with 3 K cosmic microwave background and 3 K extragalactic.

[c] Continuum all in front of H I.

4. THE D/H ABUNDANCE IN THE GALACTIC ANTICENTER

Our most significant detection is at $l = 183°$, which is the source with the largest 21 cm hydrogen line opacity because of the extreme velocity crowding in this direction. Our best estimate of the D/H ratio in this region is $(2.3 \pm 0.4) \times 10^{-5}$ ($1\,\sigma$ errors) assuming a uniform spin temperature of 130 K and uniform mixing of Galactic continuum along the line of sight. The regions centered at $l = 171°$ and $l = 195°$ have marginal detections of the D line with derived D/H ratios, based on the same model, of $(1.5 \pm 0.5) \times 10^{-5}$ and $(1.7 \pm 0.8) \times 10^{-5}$, respectively. The weighted mean for all three regions is $(2.1 \pm 0.3) \times 10^{-5}$. If we include in the uncertainty a spin temperature range of 110–150 K (see Table 3) and increase the errors from $1\,\sigma$ to $3\,\sigma$, then our D/H ratio estimate from $l = 183°$ is $2.3^{+1.5}_{-1.3} \times 10^{-5}$.

5. DISCUSSION

Ultraviolet absorption measurements of stars within 100 pc of the Sun by the *Far Ultraviolet Spectroscopic Explorer* (*FUSE*) and *Hubble Space Telescope* (*HST*) yield D/H ratios close to 1.5×10^{-5}, but the D/H ratios derived for more distant objects show a large variation. Many *FUSE* abundances for more distant objects are about a factor of 2 lower at $\sim 8 \times 10^{-6}$ (Wood et al. 2004). Quasar lines of sight (Kirkman et al. 2003) and some Galactic disk directions, however, have D/H ratios of about 2.5×10^{-5}, which is consistent with the D/H ratio derived from the baryon density implied by the *Wilkinson Microwave Anisotropy Probe* (*WMAP*) data (Spergel et al. 2003). The lower D/H abundance in the vicinity of the Sun (Wood et al. 2004) is likely due to the destruction of D by astration. The large variations of the D/H ratio are thought to be the result of preferential absorption of D onto grains (Draine 2004). Thus, undisturbed regions of the interstellar gas may be depleted of D whereas regions that have been shocked may have a D/H ratio closer to the primordial value divided by the astration factor. Our value of 2.3×10^{-5} is close to the cosmological prediction of 2.5×10^{-5} from *WMAP* data. Our conservative upper limit of 3.8×10^{-5} is consistent with the UV determinations, which sample many more lines of sight than our measurements probe. Finally, we estimate that the column density–weighted mean distance of the anticenter D-emitting gas is $\sim$2 kpc. Thus our lower limit D/H ratio of 1.0×10^{-5}, which is higher than the 8×10^{-6} from the *FUSE* and *HST* measurements for the most distant sources, raises the possibility that there could be systematic errors in either the optical or radio measurements, since the D in the anticenter direction is distributed over a path length as long as any of the measured optical paths. We plan to continue observing the anticenter to reduce the measurement error and then to tilt the stations so we can observe the Galactic center, where we would expect to see the 327 MHz line in absorption.

We thank Bruce Whittier, Richard Jackson, and the technical staff of the observatory for their contributions in the construction of the array. We also thank Preethi Pratap of the observatory staff and Marcos Diaz of Boston University for their work in the development of the RFI monitor. Support for the array came from the National Science Foundation (grant AST 01-15856), MIT, and TruePosition, Inc.

REFERENCES

Anantharamaiah, K., & Radhakrishnan, V. 1979, A&A, 79, L9
Blitz, L., & Heiles, C. 1987, ApJ, 313, L95
Burles, S., Nollett, K. M., & Turner, M. S. 2001, ApJ, 552, L1
Cesarsky, D. A., Moffet, A. T., & Pasachoff, J. M. 1973, ApJ, 180, L1
Chengalur, J. N., Braun, R., & Burton, W. B. 1997, A&A, 318, L35
Draine, B. T. 2004, BAAS, 205, No. 162.01
Ewen, H. I., & Purcell, E. M. 1951, Nature, 168, 365
Field, G. B. 1958, Proc. IRE, 46, 240
French, D. K., & Osborne, J. L. 1976, MNRAS, 177, 569
Gould, R. J. 1994, ApJ, 423, 522
Hartmann, D., & Burton, W. B. 1997, Atlas of Galactic Neutral Hydrogen (Cambridge: Cambridge Univ. Press)
Haslam, C. G. T., Salter, C. J., Stoffel, H., & Wilson, W. E. 1982, A&AS, 47, 1
Heiles, C., McCullough, P. R., & Glassgold, A. E. 1993, ApJS, 89, 271
Kirkman, D., Tytler, D., Suzuki, N., O'Meara, J. M., & Lubin, D. 2003, ApJS, 149, 1
Pasachoff, J. M., & Cesarsky, D. A. 1974, ApJ, 193, 65
Rogers, A. E. E., Pratap, P., Carter, J. C., & Diaz, M. 2005, Radio Sci., 40, RS5S17
Rogers, A. E. E., Pratap, P., Kratzenberg, E., & Diaz, M. 2004, Radio Sci, 39, RS2023
Spergel, D. N., et al. 2003, ApJS, 148, 175
Wood, B. E., Linsky, J. L., Hébrard, G., Williger, G. M., Moos, H. W., & Blair, W. P. 2004, ApJ, 609, 838
Weinreb, S. 1962, Nature, 195, 367
Wineland, D. J., & Ramsey, N. F. 1972, Phys. Rev. A., 5, 821